PEDS Advance Access published September 11, 2014

Protein Engineering, Design & Selection pp. 1–8, 2014
doi:10.1093/protein/gzu036

The disordered region of *Arabidopsis* VIP1 binds the *Agrobacterium* VirE2 protein outside its DNA-binding site

Michal Maes[1,2], Einav Amit[1], Tsafi Danieli[3], Mario Lebendiker[3], Abraham Loyter[2] and Assaf Friedler[1,4]

[1]Institute of Chemistry, The Hebrew University of Jerusalem, Safra Campus, Givat Ram, Jerusalem 91904, Israel, [2]Department of Biological Chemistry, Alexander Silberman Institute of Life Sciences, The Hebrew University of Jerusalem, Safra Campus, Givat Ram, Jerusalem 91904, Israel and [3]Wolfson Centre for Applied Structural Biology, The Hebrew University of Jerusalem, Safra Campus, Givat Ram, Jerusalem 91904, Israel

[4]To whom correspondence should be addressed.
E-mail: assaf.friedler@mail.huji.ac.il

Received July 24, 2014; revised July 24, 2014; accepted July 28, 2014

Edited by Gideon Schreiber

Agrobacterium **is a pathogen that genetically transforms plants. The bacterial VirE2 protein envelopes the T-DNA of** ***Agrobacterium*** **and protects it from degradation. Within the transfected cells, VirE2 interacts with the plant VIP1 leading to nuclear transport of the T-DNA complex. Active VirE2 is an oligomer with a tendency to aggregate, hampering its studies at the molecular level. In addition, no structural or quantitative information is available regarding VIP1 or its interactions. The lack of information is mainly because both VIP1 and VirE2 are difficult to express and purify. Here, we present the development of efficient protocols that resulted in pure and stable His-tagged VIP1 and VirE2. Circular dichroism spectroscopy and computational predictions indicated that VIP1 is mostly intrinsically disordered. This may explain the variety of protein–protein interactions it participates in. Size exclusion chromatography revealed that VirE2 exists in a two-state equilibrium between a monomer and an oligomeric form. Using the purified proteins, we performed peptide array screening and revealed the binding sites on both proteins. VirE2 binds the disordered regions of VIP1, while the site in VirE2 that binds VIP1 is different from the VirE2 DNA-binding site. Peptides derived from these sites may be used as lead compounds that block** ***Agrobacterium*** **infection of plants.**

Keywords: *Agrobacterium*/peptide arrays/protein expression and purification/VIP1/VirE2

Introduction

Agrobacterium tumefaciens is a soil-borne, Gram-negative bacterium that causes the Crown-Gall disease in plants. The transfer of a bacterial DNA segment (T-DNA) into the host plant cell is followed by its integration into the host genome and the expression of the bacterial genes resulting in neoplastic growth (Pitzschke and Hirt, 2010a). The *Agrobacterium* T-complex, which includes the bacterial VirE2 protein and the bacterial T-DNA, hijacks the plant VIP1 protein in order to facilitate its nuclear import (Pitzschke and Hirt, 2010b). The VirE2 protein protects the T-DNA from degradation by cellular nucleases (Tzfira and Citovsky, 2002). The cellular VIP1 serves as a molecular link between VirE2, the 'coat protein' of the T-complex, and plant proteins necessary for integration. It also mediates binding of this complex to the nuclear import receptor importin α (Tzfira and Citovsky, 2000, 2002; Tzfira *et al.*, 2001; Citovsky *et al.*, 2004) allowing nuclear import of the T-complex. Within the nucleus VIP1 links the T-complex to the bacterial VirF (Tzfira *et al.*, 2004; Lacroix *et al.*, 2008) or to the plant VBF protein (part of the proteosomal degradation machinery) (Zaltsman *et al.*, 2010). This interaction leads to destabilization of VirE2 and its removal from the T-DNA, thus enabling integration of the resulting naked DNA into the plant genome.

VIP1 belongs to a subfamily of plant bZIP proteins (Tzfira *et al.*, 2001). It contains a predicted basic leucine zipper (bZIP) motif (VIP1 177–291) characterized by a lysine instead of an arginine (K212 in VIP1) (Pitzschke *et al.*, 2009). Members of this family are predicted to form homodimers (Deppmann *et al.*, 2006). Indeed, homodimerization of VIP1 has been confirmed by co-immunoprecipitation and bimolecular fluorescence complementation experiments (Li *et al.*, 2005). VIP1 acts as a transcription factor under stress conditions, e.g. plant growth in sulfur-deficient environment (Wu *et al.*, 2010) or as a substrate of the MAPK-signaling pathways, which is one of the plant defense mechanisms against pathogens (Pitzschke and Hirt, 2010b). It targets a specific motif in the promoters of stress genes, termed the VIP1 response element motif (Pitzschke *et al.*, 2009). The basic region of the bZIP domain contains a classical nuclear localization signal sequence corresponding to VIP1 residues 199–217 (KRILANRQSAARSKERKIR) (Tzfira and Citovsky, 2001). The central part of VIP1 (VIP1 81–244) was shown to support nuclear import of VirE2 (Li *et al.*, 2005) and is important for intranuclear localization as well as for VirE2 binding. No information regarding the molecular structure of VIP1 is available mainly due to the inability to express and purify this protein in the amounts required for such structural studies.

The bacterial VirE2 protein is a single-stranded DNA (ssDNA)-binding protein of 63.3 kDa, encoded by the *vir* region located within the Ti plasmid of *Agrobacterium*. The C-terminal part of VirE2 is necessary for the cooperative and non-specific ssDNA-binding property of the protein (Dombek and Ream, 1997). Packaging of the T-DNA by VirE2 results in the formation of semi-rigid, hollow, cylindrical filaments with a coiled structure, providing protection from cellular nucleases and facilitating nuclear import (Tzfira and Citovsky, 2002). VirE2 is transferred from the *Agrobacterium* into the plant cytoplasm in complex with VirE1 (Sundberg *et al.*, 1996), which is a small protein of 63 residues that acts as a chaperone

and prevents aggregation of VirE2. The crystal structure of VirE2 in complex with VirE1 (Dym *et al.*, 2008) shows that VirE2 has two domains with a similar structure, in spite of a very low sequence homology. These domains are interconnected by a flexible linker (residues 337–346) that allows them to fold around the helical VirE1. The VirE1–VirE2 interaction is mainly electrostatic. VirE1 has an overall negative charge, allowing it to fit into the positively charged pocket created between the two VirE2 domains. ssDNA displaces VirE1 from VirE2 (Duckely *et al.*, 2005; Frenkiel-Krispin *et al.*, 2007), therefore it appears that the DNA-binding site of VirE2 is the same positively charged region located between both VirE2 domains. This linker region grants the conformational flexibility required to allow the different binding partners to interact. The two terminal regions (VirE2 1–111 and VirE2 517–556) seem to be unstructured.

The VIP1–VirE2 interaction was demonstrated in plant cells by immunostaining (Tzfira *et al.*, 2001; Lacroix *et al.*, 2008) and by bimolecular fluorescence complementation assay with cYFP and nYFP-tagged proteins (Li *et al.*, 2005). These assays are based on co-localization of the two proteins, but do not necessarily indicate a direct interaction between them (Kerppola, 2006; Zamyatnin *et al.*, 2006). No information on the interaction at the molecular level is currently available mainly because of the lack of purified VIP1 and VirE2 at high enough concentrations, since efficient expression and purification protocols are so far unavailable. Here we present new protocols for the expression and purification of both proteins, which allowed studying the interaction between them at the molecular level. We found that VIP1 is partially disordered, while VirE2 exists in a dynamic two-state equilibrium between a monomer and a high-order oligomer. Peptide array screening revealed the binding site between these two proteins and showed that the disordered part of VIP1 interacts with VirE2 outside its DNA-binding site.

Materials and methods

Plasmid construction

Plasmids encoding full-length His-tagged VIP1 and His-tagged VirE2 in pET28 vectors were a kind gift from Prof. Vitaly Citovsky, State University of New York, Stony Brook, New York, USA. The protein encoding sequences of these plasmids were amplified by PCR using the following oligonucleotides: CGCGGATCCatggaaggaggaggaagaggacc (VIP1-Forward primer, BamHI restriction site underlined); atggatttca ccaagagaggctgaCTCGAGCGG (VIP1-Reverse primer, XhoI restriction site underlined); ATAAGAATGCGGCCGCTgatcc gaaggccgaggc (VirE2-Forward primer, NotI restriction site underlined) and ggcccaaccgtaaacagtctgtagCTCGAGCGG (VirE2-Reverse primer, XhoI restriction site underlined). Following

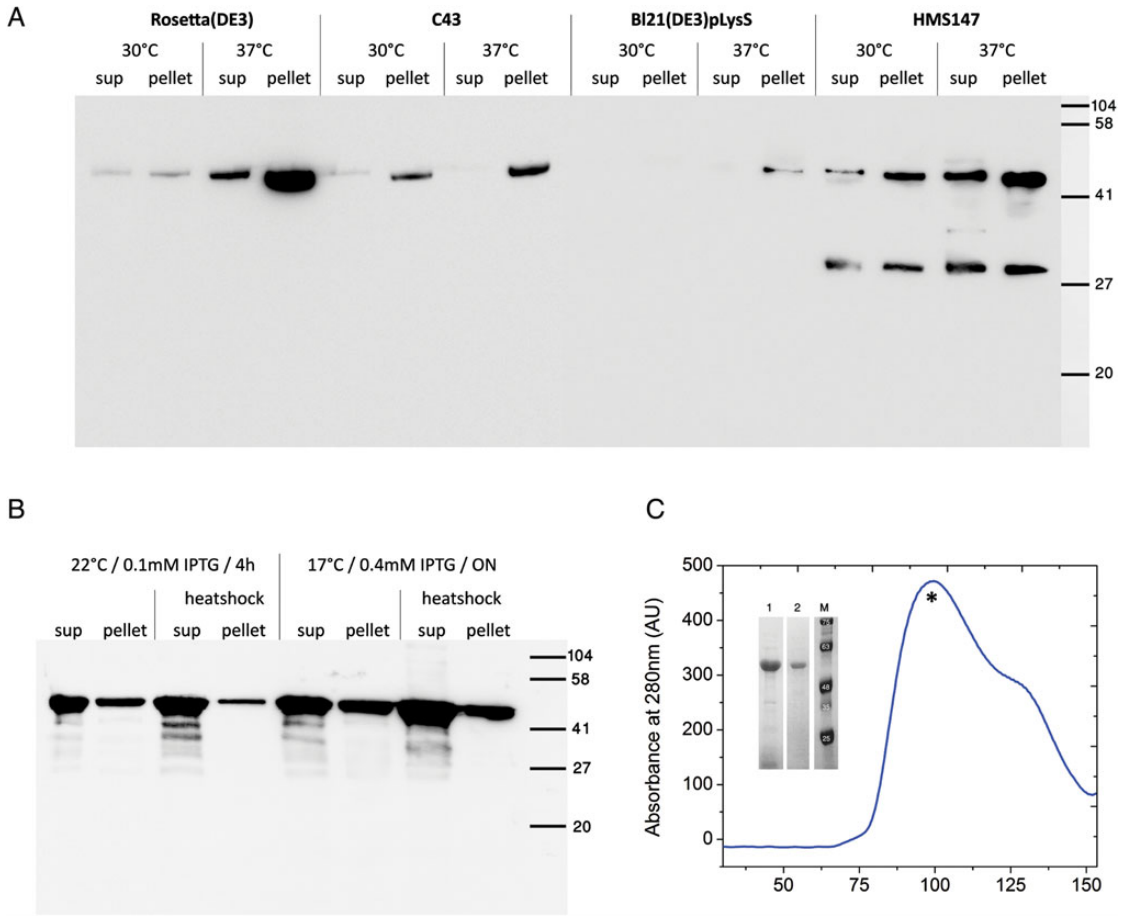

Fig. 1. HLT–VIP1 purification. (**A**) Screening of different bacterial strains for protein expression at 30 and 37°C. Soluble (S; sup) and insoluble (P; pellet) fractions were separated by centrifugation and analyzed by western blot with anti-His antibody. (**B**) Screening of induction conditions for HLT–VIP1 included heat shock treatment of the bacteria. (**C**) The final purification step was SEC using a Superose 12 column. Inset: Sodium dodecyl sulfate polyacrylamide gel electrophoresis analysis of the protein after Ni purification (lane 1) and of the main peak of SEC, marked by * on the chromatogram (lane 2).

digestion of the PCR product and pET–HLT (Siman *et al.*, 2011; Lebendiker and Danieli, 2014) by the corresponding restriction enzymes, the protein gene was ligated into the pET–HLT plasmid by using T4 DNA ligase (Takara, Shiga, Japan). The ligated vector was transformed into Top10 bacterial strain, and the resulting colonies were screened by PCR and verified by sequencing (Center for Genomic Technologies, Hebrew University).

Protein expression

The pET–HLT–VIP1 construct was transformed into Rosetta (DE3) (EMD-Novagen). The pET–HLT–VirE2 plasmid was transformed into BL21CodonPlus RP (Stratagene). Both proteins were then expressed using the same protocol: transformed bacteria were plated on ampicillin-selective plates and incubated at 37°C. After 18 h of incubation, colonies were transferred to 2×YT medium (4 ml) containing ampicillin (33 mg/l) and the culture was grown for an additional 16 h in an incubator shaker at 37°C. The grown cultures were diluted 1 : 100 into a flask containing 2×YT medium supplemented with antibiotics and the culture was grown at 37°C until OD600 reached 0.7. Bacteria transformed with pHLT–VIP1 were subjected to 42°C for 20 min after addition of 0.1% glycerol and 0.1 mM potassium glutamate. The flask was transferred into a 17°C shaker, and induced with 0.4 mM Isopropyl β-D-1-thiogalactopyranoside (IPTG). Cells were harvested 16 h post-induction, collected by centrifugation and stored at −70°C.

HLT–VIP1 purification

Pellets of HLT–VIP1-expressing bacteria were resuspended in lysis buffer (50 mM Hepes pH 8.0, 500 mM NaCl, 10% glycerol and 1 M urea) at 1 : 10 (v/v) ratio. Lysozyme (Sigma), DNase (Sigma), PMSF (Sigma) and Protease Inhibitors Cocktail (Sigma) were added according to the manufacturer's instructions. Cells were disrupted by sonication and cell debris was removed by centrifugation. The cell lysate was added to equilibrated Ni-NTA beads (Qiagen) at a 1 : 100 ratio (v/v). After incubation at 4°C for 2 h, the beads were washed twice with 20 ml wash buffer (50 mM Hepes pH 8.0, 500 mM NaCl, 10% glycerol, 1 M urea and 10 mM imidazole) and then incubated for 15 min with elution buffer (50 mM MES pH 6.0, 500 mM NaCl, 10% glycerol and 500 mM imidazole). To increase protein purity, a second purification step was performed using a 200-ml Superose 12 size exclusion chromatography (SEC) column, pre-equilibrated with the storage buffer (50 mM MES pH 6.0, 500 mM NaCl and 10% glycerol). The fractions containing pure protein were pooled, concentrated, quantified, aliquoted and stored at −70°C.

HLT–VirE2 purification

Pellets of HLT–VirE2-expressing bacteria were resuspended in lysis buffer (50 mM Hepes pH 8.0, 500 mM NaCl and 10% glycerol) at 1 : 10 (v/v) ratio. Lysozyme (Sigma), DNase (Sigma), PMSF (Sigma) and Protease Inhibitors Cocktail (Sigma) were added according to the manufacturer's instructions. Cells were disrupted by sonication and cell debris was removed by centrifugation. The cell lysate was added to equilibrated Ni-NTA beads (Qiagen) at a 1 : 100 ratio (v/v). After incubation at 4°C for 2 h, the beads were washed twice with 20 ml wash buffer (50 mM Hepes pH 8.0, 500 mM NaCl, 10% glycerol and 10 mM imidazole) and then incubated for 15 min with elution buffer (50 mM MES pH 6.0, 500 mM NaCl, 10% glycerol and 500 mM imidazole). To increase the protein purity, a second purification step was performed using a 200-ml Superose 12 SEC column, pre-equilibrated with the storage buffer (50 mM MES pH 6.0, 500 mM NaCl and 10% glycerol). The fractions containing pure protein were pooled, concentrated, quantified, aliquoted and stored at −70°C.

Structure predictions

The full-length VIP1 sequence was subjected to disorder prediction using the server default parameters. The following servers were used: DisPro (Cheng *et al.*, 2005), DisoPred (Ward *et al.*, 2004), DisEMBL loop/coil, DisEMBL hotloops, DisEMBL465 (Linding *et al.*, 2003a), GlobProt (Linding *et al.*, 2003b), DripPred (Ferron *et al.*, 2006) and NORSS (Liu and Rost, 2003).

Circular dichroism

Circular dichroism (CD) spectra were recorded using a J-810 spectropolarimeter (Jasco) in 0.1 cm quartz cuvettes. Far UV spectra were collected for 9 μM HLT–VIP1 over 190–260 nm at 10°C. Control experiments were performed with HLT under similar conditions.

Size exclusion chromatography

Analytical SEC of the proteins was performed on an AKTA design Explorer instrument equipped with a Monitor UV-900

Table I. The new protein production protocols compared with the previous protocols

(A) *Arabidopsis* VIP1		
	Previous protocol (Lacroix *et al.*, 2008)	Our protocol
Plasmid encoding	His-tagged VIP1	HLT–VIP1
Expression in	BL21(DE3)pLysS	Rosetta(DE3)
Expressed protein	In inclusion bodies	Soluble protein
Purification	Denaturation with 4 M urea Renaturation on Ni (bench) Dialysis	Ni binding in batch SEC
Concentration determination	No Trp—no ε By Bradford's assay (Bradford, 1976)	$\varepsilon = 12\,950\ M^{-1}\ cm^{-1}$ By UV spectroscopy
Final buffer	10 mM Phosph pH8.0 100 mM NaCl 10% glycerol 1 mM PMSF 1 mM βMe	50 mM MES pH6.0 500 mM NaCl 10% glycerol
Maximal concentration	2 μM	20 μM
(B) *Agrobacterium* VirE2		
	Previous protocol (Frenkiel-Krispin *et al.*, 2007; Dym *et al.*, 2008)	Our protocol
Plasmid encoding	Selenomethionine labeled VirE2-VirE1	HLT–VirE2
Expression in	BL21(DE3)	BL21CodonPlusRP
Expressed protein	In inclusion bodies	Soluble protein
Purification	Denaturation with 5 M urea Refolded by dialysis Ceramic hydroxyapatite column SEC	Ni binding in batch SEC
Final buffer	20 mM Tris pH8.0 50 mM NaCl 1 mM DTT	50 mM MES pH6.0 500 mM NaCl 10% glycerol
Maximal concentration	115 μM In complex with VirE1	40 μM HLT-tagged VirE2

detector and the Unicorn software package using a Superose 12 analytical column (~4 ml, GE Healthcare-Pharmacia Corp.) equilibrated with a buffer (50 mM MES, pH 6.0, 500 mM NaCl and 10% glycerol). Proteins were eluted with a flow rate of 0.4 ml/min and the elution profile was monitored by UV absorbance at 220 nm. The column was calibrated with molecular weight standards (GE Healthcare-Amersham Pharmacia).

Peptide array screening

Celluspots™ peptide arrays were purchased from Intavis (Cologne, Germany). The array was blocked for 4 h at room temperature with 5% skimmed milk in phosphate buffered saline with Tween-20 (PBS-T). The proteins were diluted in 5% skimmed milk in PBS-T ([HLT–VIP1] = 2 μM and [HLT–VirE2] = 0.4 μM) and incubated with the array overnight at 4°C. Protein–peptide interaction was detected by using a His-probe HRP-conjugated monoclonal antibody (Santa Cruz).

Results

Expression and purification of HLT–VIP1

The previously described purification protocol for the truncated recombinant His-VIP1 includes extraction from inclusion bodies and a denaturation—refolding step (Lacroix *et al.*, 2008). To optimize the protocol and obtain higher VIP1 concentrations, we transformed different *Escherichia coli* strains with the pHLT–VIP1 plasmid. Cultures were grown in an auto-induced media (Studier, 2005) at 30 and 37°C for 16 h. Following cell lysis, the ratio of HLT–VIP1 between the soluble and insoluble fractions was determined. Western blot analysis using a HRP-conjugated anti-His antibody showed that in the traditional Bl21(DE3) pLysS strain, the 50 kDa HLT–VIP1 chimeric protein appeared only in the insoluble fraction obtained from bacteria grown at 37°C (Fig. 1A). Using the HMS147 and Rosetta (DE3) strains, the chimeric protein was observed in the soluble fractions. Expression of the pHLT–VIP1 plasmid in the HMS147 strain resulted in an additional band corresponding to a truncated protein, probably due to premature termination, and thus the Rosetta (DE3) strain was selected for further studies (Fig. 1A). Following the selection of the optimal bacterial strain, we calibrated conditions such as induction duration, temperatures and IPTG concentrations. The final induction conditions included 0.4 mM IPTG at 17°C for 16 h. We were able to further enhance the solubility of the chimeric protein by using heat shock treatment of 20 min at 42°C prior to induction (Fig. 1B). The recombinant protein was purified by affinity chromatography by the use of Ni^{2+} beads and further purified using a Superose 12 SEC column. A single peak corresponding to HLT–VIP1 was

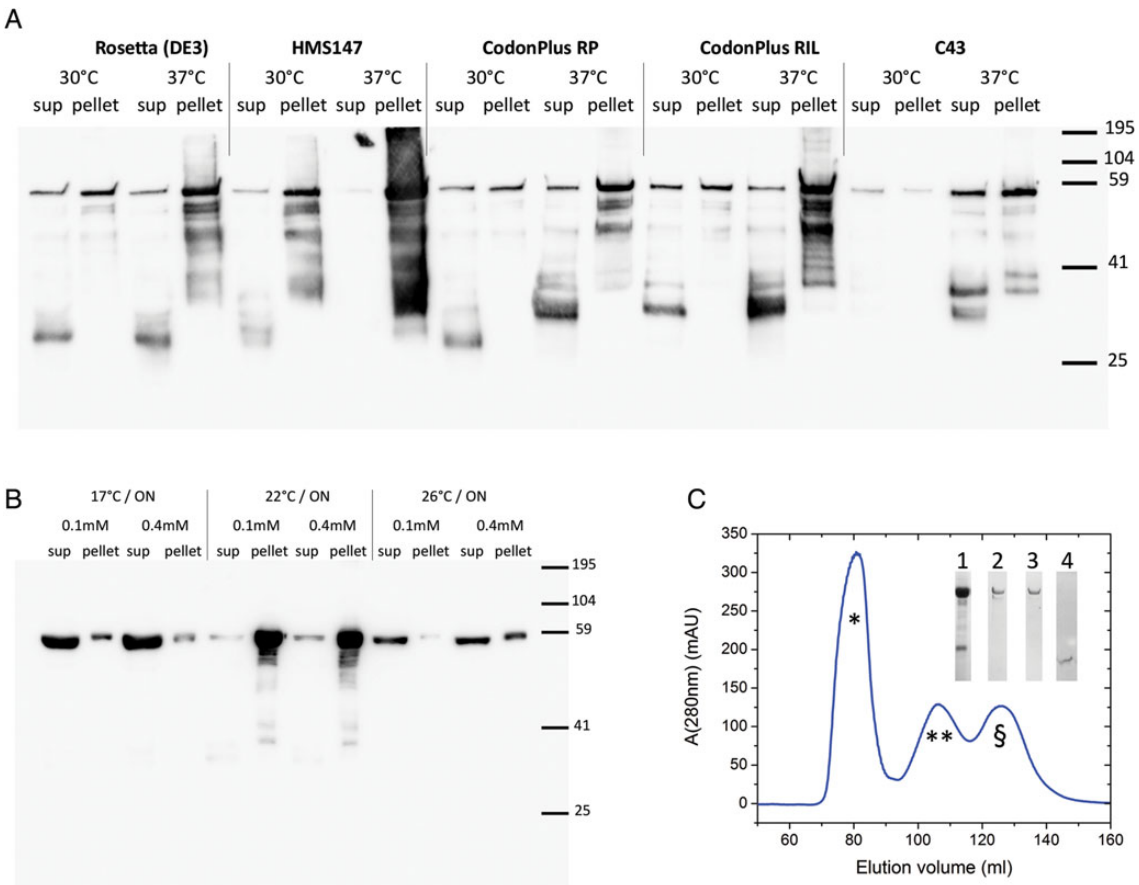

Fig. 2. HLT–VirE2 purification. (**A**) Screening of different bacterial strains for protein expression at 30 and 37°C. Soluble (S; sup) and insoluble (P; pellet) fractions were separated by centrifugation and analyzed by western blot with anti-His antibody. (**B**) Screening of induction conditions. (**C**) The final purification step was SEC using a Superose 12 column. Inset: Sodium dodecyl sulfate polyacrylamide gel electrophoresis analysis of the protein after Ni purification (lane 1) and of the three peaks after SEC (lane 2: peak marked *, lane 3: peak marked ** and lane 4, marked by § on the chromatogram).

obtained (Fig. 1C). Following this protocol, we have obtained HLT–VIP1 at a final concentration of 20 μM, which is about 10-fold higher than that was previously reported (Lacroix *et al.*, 2008). Table IA summarizes the differences between the old and new protocols and the improvements achieved in the present work.

Expression and purification of HLT–VirE2

Optimization of the expression conditions for the pHLT–VirE2 plasmid was performed essentially as described above for pHLT–VIP1. Briefly, the optimized conditions were obtained in the bacterial strain BL21CodonPlus RP and induction was performed with 0.4 mM IPTG at 17°C for 16 h (Fig. 2A and B). The protein was purified on a Ni affinity column followed by SEC using a Superose 12 column (Fig. 2C). The purified protein was concentrated to a final concentration of up to 40 μM. Table IB summarizes the differences between the old and new protocols and the improvements made in the present work.

VIP1 is partially disordered

The availability of relatively high concentration of VIP1 allowed us to analyze its structure for the first time. We submitted its sequence to several disorder prediction servers (Fig. 3A). VIP1 was predicted by most servers to be highly disordered, with the only structured region in the predicted bZIP domain (residues 177–291) (Tzfira *et al.*, 2001). The CD spectrum of the HLT–VIP1 (Fig. 3B) was characteristic of a combination of helices and unstructured regions, in agreement with the structure prediction. Analysis of the CD data using DICHROWEB (Whitmore and Wallace, 2004) quantified the results as being 40–50% helical and 50–60% random coil. The HLT-tag does not contribute to the helical content of the protein (Faust *et al.*, 2014). Analytical SEC of the pure HLT–VIP1 resulted in an elution volume that was lower than expected and the protein eluted in a wide peak (Fig. 3C). HLT–VIP1, which has the MW of 50 kDa, had an elution volume similar to the 66 kDa BSA. The difference between the elution volumes of the protein with and without urea is 0.4 ml, which is 10% of the column volume. This behavior is characteristic of disordered proteins, which are not globular and thus behave as if they were larger and have more optional conformations. Urea is a widely used protein-denaturing agent. Adding even 1 M urea resulted in the elution of the protein at a lower volume, corresponding to a more open conformation. This indicates that the protein was partially folded, and adding urea resulted in its unfolding.

VirE2 exists in dynamic equilibrium between a monomer and an oligomer

Pure HLT–VirE2 was obtained in two different fractions (Fig. 2C). The first peak is a high order oligomer while the second one corresponds to the monomeric form of the protein. Analytical SEC revealed that the pure HLT–VirE2 is in dynamic equilibrium between the monomeric form and a higher order oligomer (Fig. 4A). Dilution shifted the monomer:oligomer ratio toward the monomer (Fig. 4B).

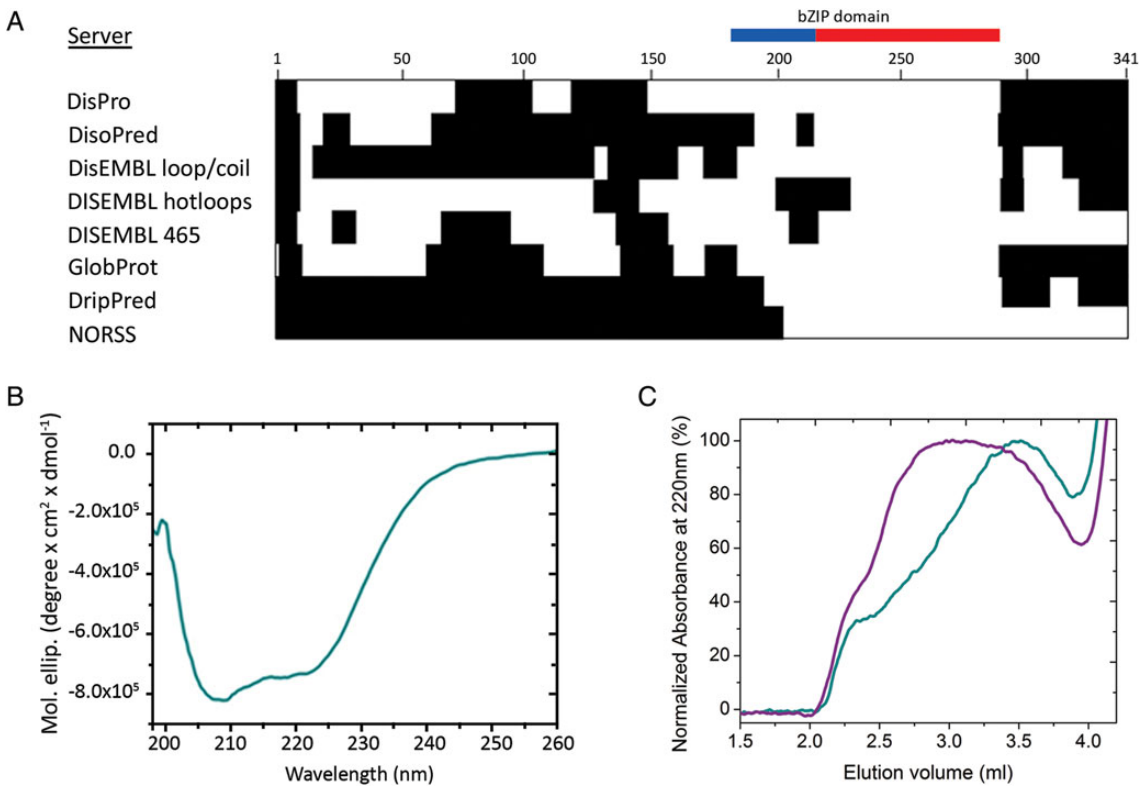

Fig. 3. VIP1 is partially disordered. (**A**) Disorder predictions were performed using 10 different algorithms (see Materials and Methods). Each row represents the disorder prediction of the VIP1 sequence by a different server. Segments that are predicted to be disordered are marked in black. The leucine zipper region, which contains a basic domain (residues 177–217, blue) and a structured α-helix (residues 218–291, red), is indicated. (**B**) The CD spectrum of HLT–VIP1 shows a combination of helices and unstructured regions. (**C**) Analytical SEC of HLT–VIP1 showed an elution volume smaller than expected (green), indicating a non-compact structure. Addition of 1 M urea to the buffer (purple) reduced the elution volume, corresponding to a more open conformation upon urea denaturation.

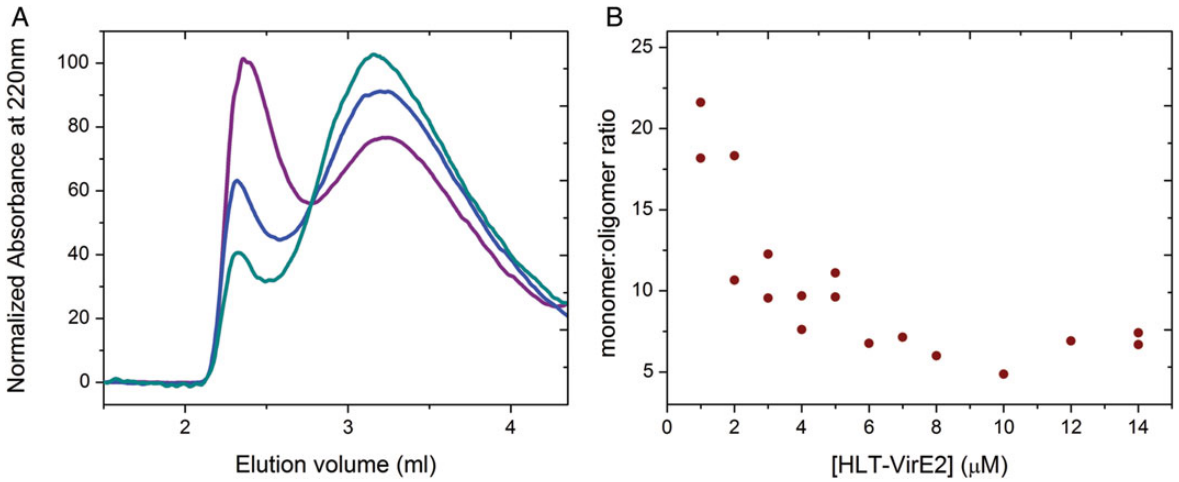

Fig. 4. VirE2 exists in a dynamic two-state oligomerization equilibrium. (**A**) Samples of 8.8 μM (purple), 4.4 μM (blue) and 1.8 μM (cyan) HLT–VirE2 were run on a mini-analytical SEC. The normalized data show a dynamic two-state equilibrium. (**B**) Monomer: oligomer ratio as a function of HLT–VirE2 concentration.

Table II. Peptide array screening reveals the VIP1–VirE2-binding site*

Peptide	Sequence	ELISA
(A) VirE2-binding peptides		
VIP1 96–110	WPNSLPPKPEARFGRH	Binding
VIP1 194–208	WDPKRAKRILANRQSA	Binding
VIP1 216–230	IRYTGELERKVQTLQ	Binding
VIP1 291–305	EIPQGNGNSYNRAQF	Binding
VIP1 329–341	PSLPSYMDFTKRG	No binding
(B) VirE2-binding peptides		
VirE2 279–293	WAGDAYANKRFEEFER	Binding
VirE2 324–338	WERGSADIRFAEFAGE	Binding

*Binding peptides as revealed by the peptide array screening. Enzyme-linked immunosorbent assay (ELISA) experiments confirmed the binding.

The VIP1–VirE2 binding site

To reveal the specific sites that mediate the interaction between VIP1 and VirE2, we performed peptide array screening (Katz *et al.*, 2011). An array containing 15-residues partly overlapping peptides derived from VIP1 81–341 and full length VirE2 was screened for binding HLT–VIP1 or HLT–VirE2 (Table II). HLT–VirE2 bound several VIP1-derived peptides (Fig. 5A) located specifically in the disordered regions of the protein. HLT–VIP1 bound only two VirE2-derived peptides (Fig. 5B) corresponding to residues VirE2 279–293 and VirE2 324–338. While these sequences are distant from each other in the primary protein sequence, they are spatially close in the protein structure and form a single continuous binding site (Fig. 5C). To confirm and quantify the peptide array screening results, we performed an enzyme-linked immunosorbent assay (ELISA)-based assay between the recombinant proteins and the array-derived binding peptides (data not shown). Almost all peptides bound the partner proteins (Table II). However, the maximum protein concentrations reached were still below the binding affinity and thus full binding curves could not be obtained and quantification was not possible.

Discussion

Here we present improved protocols for the expression and purification of HLT–VIP1 and HLT–VirE2. Using purified recombinant proteins, we were able to study the interaction between these two proteins for the first time at a molecular level. Our protocols show some important advantages compared with the protocols described before in the literature (Table I): in our protocols both proteins remain soluble during their expression and following cell lysis, making the denaturation–renaturation steps that were used before (Frenkiel-Krispin *et al.*, 2007; Dym *et al.*, 2008; Lacroix *et al.*, 2008) unnecessary. The use of HLT–VIP1 offers another benefit over the previously used VIP1: the WT protein does not contain any Trp residue but the presence of the HLT-tag adds a Trp residue that allows accurate concentration determination by UV spectroscopy. The 4 M urea used in the published protocol completely denatures the VIP1 protein from the inclusion bodies. The 1 M urea used in our protocol enhances the protein solubility during lysis, thus rescuing it from the insoluble fractions. When VIP1 was purified using the published protocol (Lacroix *et al.*, 2008) the maximal concentration that could be reached was 2 μM, while our optimized protocol yield 20 μM of pure HLT–VIP1. The crystal structure of VirE2 was solved only in complex with its chaperone VirE1 (Dym *et al.*, 2008). In order to obtain concentrations high enough for crystallization, VirE2 was co-expressed with VirE1, when both proteins were labeled with selenomethionine (Frenkiel-Krispin *et al.*, 2007). Our protocol enabled us to purify HLT-tagged VirE2 without VirE1, and reach concentrations of up to 40 μM. The final storage buffer for both proteins is more acidic than in the existing protocols, which is similar to the pH of their natural environment in the plant cells.

The strategy used to obtain the optimized protocols used here is described in detail in Lebendiker and Danieli (2014) and Lebendiker *et al.* (2014). Briefly, the methodology starts with finding optimal expression conditions by screening several bacterial strains and induction conditions (time, temperature and IPTG concentrations). Next, conditions are screened for small scale purifications. These include different buffers with different additives as well as several purification strategies.

The structure of VIP1 was predicted using multiple online servers to be partially disordered (Fig. 3A). The predicted structured part of the protein corresponds to the leucine zipper (VIP1 218–291) (Tzfira *et al.*, 2001). Our CD (Fig. 3B) results also show that the protein has a combination of disordered and

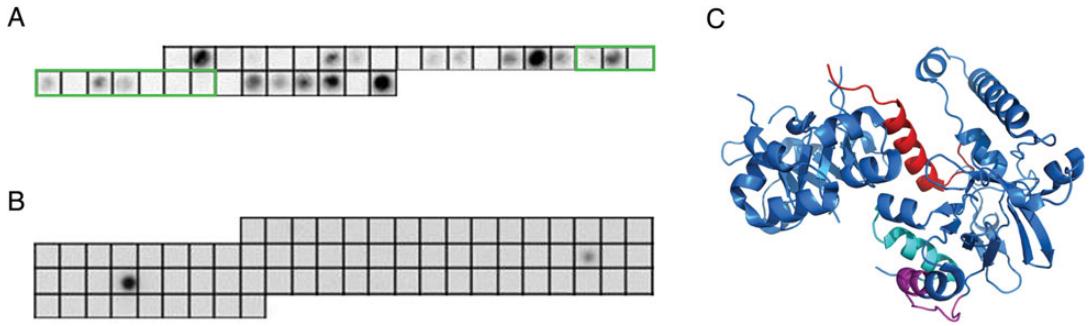

Fig. 5. The VIP1–VirE2-binding site. Peptide array screening revealed the binding sites between the two proteins (see Table II for peptide sequences). (**A**) VIP1-derived peptides that bound VirE2. Peptides derived from the structured leucine zipper (VIP1 177–217) are labeled in green. (**B**) VirE2-derived peptides that bound VIP1. (**C**) The VIP1-binding peptides (VirE2 324–338 in cyan and VirE2 279–293 in pink) on the VirE2 structure (PDB #: 3BTP; VirE2 in blue and VirE1 in red).

helical regions. Our analytical SEC results further confirm the partly disordered nature of the protein (Fig. 3C). To the best of our knowledge, this is the first experimental data on the structure of VIP1.

The bacterial VirE2 protects the T-DNA from degradation in the plant cytosol (Gelvin, 1998) by creating semi-rigid, hollow, cylindrical filaments with a coiled structure around the ssDNA (Tzfira and Citovsky, 2002). Our results show that VirE2 exists in a two-state dynamic equilibrium (Fig. 4) between the monomeric protein and an oligomeric form. This is in accordance with its biological function, since VirE2 needs to oligomerize in order to form the DNA-protecting filaments.

Using the recombinant proteins in peptide array screening and ELISA-based assays, we determined the VIP1–VirE2-binding site (Fig. 5, Table II). VirE2 bound multiple peptides, all derived from the disordered regions of VIP1. Disordered regions are well known to mediate protein–protein interactions (Reingewertz *et al.*, 2013). Only two VirE2-derived peptides bound VIP1. Though these peptides are far away in the primary sequence, they in close proximity within the VirE2 structure (Fig. 5C) creating one single binding site. This site is distinctly different from the VirE2-binding site with VirE1 and the DNA (Sundberg and Ream, 1999; Frenkiel-Krispin *et al.*, 2007; Dym *et al.*, 2008). We conclude that VIP1 binds VirE2 at region different from the DNA-binding region of VirE2.

The interaction between the bacterial VirE2 and the plant VIP1 mediates a crucial step in the infection process of plants by *Agrobacterium*. VirE2 has several important functions during the integration of the bacterial DNA into the host DNA. On the one hand, it protects the T-DNA from plant nucleases by binding it through its VirE1-binding interface (Dym *et al.*, 2008). On the other hand, VirE2 acts as a mediator between the T-complex and the plant nuclear import machinery by binding VIP1. VirE2 has to carry out both these functions simultaneously. Our findings of the VIP1-binding regions on VirE2 provide a molecular explanation for this, as the binding sites for VIP1 and the DNA are different. As the VIP1–VirE2 interaction is necessary for successful *Agrobacterium* infection, the peptides derived from the interaction interface found in this study could serve as starting points for further study of this interaction and future applications such as inhibitors.

Funding

This work was supported by a starting grant from the European Research Council under the European Community's Seventh Framework Programme (FP7/2007-2013)/ERC Grant agreement n° 203413 and by the Minerva Center for Biohybrid complex systems.

References

Bradford,M.M. (1976) *Anal. Biochem.*, **72**, 248–254.
Cheng,J.L., Sweredoski,M.J. and Baldi,P. (2005) *Data Min. Knowl. Discov.*, **11**, 213–222.
Citovsky,V., Kapelnikov,A., Oliel,S., Zakai,N., Rojas,M.R., Gilbertson,R.L., Tzfira,T. and Loyter,A. (2004) *J. Biol. Chem.*, **279**, 29528–29533.
Deppmann,C.D., Alvania,R.S. and Taparowsky,E.J. (2006) *Mol. Biol. Evol.*, **23**, 1480–1492.
Dombek,P. and Ream,W. (1997) *J. Bacteriol.*, **179**, 1165–1173.
Duckely,M., Oomen,C., Axthelm,F., Van Gelder,P., Waksman,G. and Engel,A. (2005) *Mol. Microbiol.*, **58**, 1130–1142.
Dym,O., Albeck,S., Unger,T., Jacobovitch,J., Branzburg,A., Michael,Y., Frenkiel-Krispin,D., Wolf,S.G. and Elbaum,M. (2008) *Proc. Natl Acad. Sci. USA*, **105**, 11170–11175.
Faust,O., Bigman,L. and Friedler,A. (2014) *Chem. Commun.*, **50**, 10797–10800.
Ferron,F., Longhi,S., Canard,B. and Karlin,D. (2006) *Protein Struct. Funct. Bioinformatics*, **65**, 1–14.
Frenkiel-Krispin,D., Wolf,S.G., Albeck,S., *et al.* (2007) *J. Biol. Chem.*, **282**, 3458–3464.
Gelvin,S.B. (1998) *J. Bacteriol.*, **180**, 4300–4302.
Katz,C., Levy-Beladev,L., Rotem-Bamberger,S., Rito,T., Rüdiger,S.G.D., Friedler,A. and Rudiger,S.G.D. (2011) *Chem. Soc. Rev.*, **40**, 2131–2145.
Kerppola,T.K. (2006) *Nat. Protoc.*, **1**, 1278–1286.
Lacroix,B., Loyter,A. and Citovsky,V. (2008) *Proc. Natl Acad. Sci. USA*, **105**, 15429–15434.
Lebendiker,M. and Danieli,T. (2014) *FEBS Lett.*, **588**, 236–246.
Lebendiker,M., Maes,M. and Friedler,A. (2014) *Methods Mol. Biol.* (in press).
Li,J., Krichevsky,A., Vaidya,M., Tzfira,T. and Citovsky,V. (2005) *Proc. Natl Acad. Sci. USA*, **102**, 5733–5738.
Linding,R., Jensen,L.J., Diella,F., Bork,P., Gibson,T.J. and Rusell,R.B. (2003a) *Structure*, **11**, 1453–1459.
Linding,R., Rusell,R.B., Neduva,V. and Gibson,T.J. (2003b) *Nucleic Acids Res.*, **31**, 3701–3708.
Liu,J.F. and Rost,B. (2003) *Nucleic Acids Res.*, **31**, 3833–3835.
Pitzschke,A., Djamei,A., Teige,M. and Hirt,H. (2009) *Proc. Natl Acad. Sci. USA*, **106**, 18414–18419.
Pitzschke,A. and Hirt,H. (2010a) *EMBO J.*, **29**, 1021–1032.
Pitzschke,A. and Hirt,H. (2010b) *Cell Cycle*, **9**, 18–19.
Reingewertz,T.H., Britan-Rosich,E., Rotem-Bamberger,S., *et al.* (2013) *Bioorg. Med. Chem.*, **21**, 3523–3532.
Siman,P., Blatt,O., Moyal,T., Danieli,T., Lebendiker,M., Lashuel,H.A., Friedler,A. and Brik,A. (2011) *Chembiochem*, **12**, 1097–1104.
Studier,F.W. (2005) *Protein Expr. Purif.*, **41**, 207–234.
Sundberg,C., Meek,L., Carroll,K., Das,A. and Ream,W. (1996) *J. Bacteriol.*, **178**, 1207–1212.
Sundberg,C.D. and Ream,W. (1999) *J. Bacteriol.*, **181**, 6850–6855.
Tzfira,T. and Citovsky,V. (2000) *Mol Plant Pathol.*, **1**, 201–212.
Tzfira,T. and Citovsky,V. (2001) *Mol. Plant Pathol.*, **2**, 171–176.
Tzfira,T. and Citovsky,V. (2002) *Trends Cell Biol.*, **12**, 121–129.
Tzfira,T., Vaidya,M. and Citovsky,V. (2001) *EMBO J.*, **20**, 3596–3607.
Tzfira,T., Vaidya,M. and Citovsky,V. (2004) *Nature*, **431**, 87–92.

Ward,J.J., McGuffin,L.J., Bryson,K., Buxton,B.F. and Jones,D.T. (2004) *Bioinformatics*, **20**, 2138–2319.
Whitmore,L. and Wallace,B.A. (2004) *Nucleic Acids Res.*, **32**, W668–W673.
Wu,Y., Zhao,Q., Gao,L., Yu,X.-M., Fang,P., Oliver,D.J. and Xiang,C.-B. (2010) *J. Exp. Bot.*, **61**, 3407–3422.
Zaltsman,A., Krichevsky,A., Loyter,A. and Citovsky,V. (2010) *Cell Host Microbe*, **7**, 197–209.
Zamyatnin,A.A., Solovyev,A.G., Bozhkov,P.V., Valkonen,J.P.T., Morozov,S.Y. and Savenkov,E.I. (2006) *Plant J.*, **46**, 145–154.